CONF-810809--32

CONF-810809--32

DE83 008507

STUDY OF COEXISTENCE OF FERROMAGNETISM AND SUPERCONDUCTIVITY IN SINGLE-CRYSTAL $ErRh_4B_4$

S. K. Sinha, G. W. Crabtree and D. G. Hinks

Argonne National Laboratory, Argonne, Illinois 60439

and

H. Mook

Oak Ridge National Laboratory, Oak Ridge, Tennessee†

ABSTRACT

Neutron diffraction and resistivity measurements on single crystals of $ErRh_4B_4$ have revealed that both superconductivity and ferromagnetic order coexist in this material between 0.71 K and 1.2 K. In this intermediate phase, a linear polarized modulated structure with a wavelength of approximately 100 Å is observed. The modulated moment increases faster than the ferromagnetic moment down to 0.71 K and then disappears suddenly, with loss of superconductivity and a transition to a normal ferromagnetic state. This transition is accompanied by temperature hysteresis of about 60 mK. The same hysteresis, in the inverse sense, is exhibited by the ferromagnetic component. We interpret the intermediate phase as being one of coexisting normal ferromagnetic domains and superconducting sinusoidally ordered domains. Evidence of a small percentage of small ferromagnetic regions of size ~ 100 Å is also seen in both the intermediate and ferromagnetic phases.

*Work supported by the U.S. Department of Energy.
†Research sponsored by the Division of Materials Science, U.S. Department of Energy under contract W-7405-Eng-26 with the Union Carbide Corporation.

Recent studies of several superconducting materials which contain a lattice of magnetic ions [1-7] have revived interest in the problem of the coexistence of superconductivity and long range magnetic order. While it is clear that antiferromagnetic long range order can coexist with superconductivity [6], the situation is not quite as clear in the case of ferromagnets, such as $ErRh_4B_4$. Several experiments have been performed on polycrystalline samples of $ErRh_4B_4$, including bulk magnetic and transport measurements [1-3], and Mössbauer [4] and neutron diffraction [5,7] studies. Early measurements indicated that, in zero external magnetic field, $ErRh_4B_4$ exhibits a superconducting transition at 8.7 K (T_{c_1}) and then orders ferromagnetically with apparent loss of superconductivity at approximately 0.9 K (T_{c_2}), with some hysteresis at the lower transition. Blount and Varma [8] considered the competition between tendencies to ferromagnetism and superconductivity and predicted the occurrence of an intermediate spirally ordered magnetic state, still in the superconducting phase, followed at lower temperatures by a first-order transition to a normal ferromagnetic state. On the other hand, other authors [9-11] obtained the result that the intermediate state was a vortex lattice, which at lower temperatures, may undergo a further transition to a purely ferromagnetic normal state. Greenside et al. [12] considered the effect of magnetic anisotropy, and generalized the Blount-Varma spiral state to include the possibility of a linearly polarized sinusoidal state. They rule out the vortex intermediate state as having too high a free energy relative to the purely sinusoidal states. Recent small-angle neutron diffraction studies by Moncton et al. [7] on a powder sample show the growth of a peak at Q = 0.06 $\AA^{-1}$ at temperatures below 1.1 K and a rapid decrease of the peak intensity below 0.65 K. They observed that the peak exhibits temperature hysteresis, which is mirrored in a complementary fashion by the ferromagnetic Bragg peak intensity. These authors concluded that the small-angle peak corresponds to a modulated structure of the type proposed by Blount and Varma, with a wavelength of ~ 100 Å. Similar long wavelength oscillatory moment components have been recently observed also at the superconducting to ferromagnetic (SC/FM) transition in $HoMo_6S_8$ [13].

The present studies were carried out on a single crystal of $ErRh_4B_4$ grown from an Er-Rh-B melt. The right was found to consist of two single crystal grains, the larger of which, being a mass of ~ 0.3 gms, was used for the neutron diffraction studies. The other grain was used for the re-sis-tivity measurements. The neutron diffraction sample was mounted with the [010] axis vertical inside a pumped ^{3}He refrigerator on the HB2 spectrometer at the HFIR Reactor. The sample was found to have a mosaic spread of ~ 10' arc. Most scans were carried out in a double-axis mode with an incident neutron wavelength of 2.35 Å and an incident collimation of 40'. Studies were made around the (200), (101), (102) and (002) reciprocal lattice points. A comparison of integrated rocking curve intensities of the purely nuclear reflections in the paramagnetic phase at 1.5 K showed that the nuclear structure factors of the (101) and (102) reflections were consistent within 1% of those expected from the crystal structure. These two reflections had the most similar geometrical configurations for the sample crystal in the neutron beam. The integrated intensities of the (200) and (002) nuclear Bragg peaks indicated a necessity for making corrections (9% and 46%, respectively) for the high absorption in the sample. Integrated intensities for other nuclear reflections such as the (004) and (103), which have nuclear structure factors greater by two orders of magnitude compared to the innermost reflections, indicated considerable extinction for these reflections. Thus only the intensities of the innermost reflections were used for an analysis of the data. The procedure adapted was to measure the observed magnetic peak intensities relative to the corresponding nuclear peak intensities and obtain magnetic structure factors from the known nuclear structure factors. It is, however, likely that the strong ferromagnetic intensities [particularly at the (002) reflection] at the lowest temperatures are affected by extinction, and thus preclude an accurate determination of the ordered ferromagnetic moment.

For $T < 1.2$ K, ferromagnetic intensity was observed at the (200), (101) and (002) reflections but not at (102), as expected from structure factor considerations. Four satellite peaks were also observed around (200), (101) and (002) in the a*-c* plane at positions ($\pm 0.042\ \vec{a}^* \pm 0.055\ \vec{c}^*$). These positions form an almost perfect square in reciprocal space. Weak additional satellites seen at ($\pm 0.055\ \vec{c}^*$) around (101) and (002) were ascribed to a similar set of satellite peaks in the equivalent vertical a*-c* plane, picked up by the relaxed vertical diffractometer resolution. These satellites were not picked up around (200).

Figure 1 shows the temperature dependence of the (101) ferromagnetic and satellite intensities. The satellite positions indicate sinusoidally modulated magnetic structures with propagation directions at 45° to the [001] and each of the [100] and [010] axes, with a wavelength of 91.8 Å. Figure 2 shows a high resolution scan taken at 0.7 K of one of the satellite peaks, and it is seen that no significant peak width is seen beyond instrumental resolution. The same was true of the ferromagnetic peaks. From such scans we may conclude that at this temperature both the ferromagnetic and satellite peaks correspond to magnetically ordered regions coherent over at least 2400 Å. The periodicity of the modulated moment showed only a very slight temperature dependence increasing to 103.6 Å at 0.97 K. No higher order satellites were found in spite of careful scans to search for them, to within an estimated threshold of 2% of the main satellite intensities. Figure 1 shows that the modulated moment disappears suddenly on cooling below 0.7 K and reappears suddenly on warming back to 0.775 K. This indicates a first order transition. The satellite intensity is mirrored in the opposite sense by the behavior of the ferromagnetic intensity as seen in Fig. 1. The intensity curves were quite reproducible, provided one warmed or cooled well beyond T_M or T_{c_2}, respectively. In addition, there appeared to be a sluggish time response of the intensities to large temperature changes and a few minutes elapsed before equilibrium appeared to be established. Figure 1 also shows the temperature dependence of the bulk d.c. resitivity. This establishes that the modulated moment disappears and reappears with bulk superconductivity in the sample. The small differences in the transition temperatures observed by the two techniques are probably due to a slight (~ 20 mK) non-reproducibility in the temperature of the resistive transition. In spite of this non-reproducibility, the magnitude, sharpness, and hysteresis of the transition were constant from measurement to measurement.

The temperature dependence of the ferromagnetic intensity does not follow the conventional behavior below T_m. In fact, although the peak is quite sharp in reciprocal space, it is more suggestive of critical scattering. This is reminiscent of the "central mode" critical scattering seen at the structural phase transition in $SrTiO_3$ [14]. Another possibility is that the ferromagnetic scattering near T_m comes from only a small fraction of the sample. As the temperature is lowered, these ferromagnetic regions grow in size, forcing the intensity to grow faster than the square of the ordered moment.

At lower temperatures, a broad diffuse component appears around each ferromagnetic reflection. This could not be fitted with the usual Lorentzian profile as might arise from short-range order effects. However, the intensity profile near a Bragg reflection could be well fitted with the sum of a sharp Gaussian (representing the Bragg peak) and a smaller broad Gaussian scattering function, folded with the instrumental resolution function. Such a broad Gaussian is characteristic of small ferromagnetic regions. Figure 3 shows a typical fit to the magnetic intensity observed in one of the scans near (but not through) the (101) reciprocal lattice point. Typical of these scans is the asymmetry of the broad diffuse ponent, which is satisfactorily reproduced in the fits. The broad component was observed both in the intermediate phase ($T_{c_2} < T < T_m$) and in the purely ferromagnetic phase, and yielded a rms value for the full width at half maximum of the small ferromagnetic domains of ~ 100 Å. The volume of such regions (as estimated from the ratios of integrated intensities), is only 9% of the ferromagnetic regions at 0.75 K, and ~ 5% at T = 0.54 K. These small ferromagnetic regions, which must be incoherent with the main ferromagnetic regions, may arise from domain walls, as already suggested by Moncton et al. [7]. Another possibility is small <u>disordered</u> regions of size 100 Å inside the large coherent ferromagnetic regions.

Finally, we turn to the quantitative analysis of the intensity data and the nature of the intermediate state. Table I lists the squares of the magnetic structure factor for the observed ferromagnetic reflections at three different temperatures below T_m. They are consistent within experimental error with a uniform ferromagnetic structure with the moment along the (vertical) [010] axis. This is somewhat surprising, since one would expect equally populated ferromagnetic domains with moments along <u>each</u> equivalent a-axis, but may be due to effects induced by slight stresses arising from each mounting. If so, it shows that the magnetic anisotropy in the "easy" plane is extremely weak. Also shown are the deduced value for the ordered ferromagnetic moment/Er atom, although the lowest temperature value is probably too low owing to extinction effects. The powder diffraction data value of 5.6 μ_B/Er atom for the saturated ferromagnetic moment [5] is probably more reliable. We also show in Table 1, $|F_{mag}|^2$ for one particular satellite as observed from around the (200), (101) and (002) positions. The result is consistent with a linearly polarized sinusoidal modulation along with the [010] axis, i.e., it is transversely polarized. Consistent with this is the absence of the equivalent satellites in the vertical c*-a* plane around the (200) reflection, since these would have their moment direction along [100].

Figure 1 shows the ratio of the intensity (I_S) of the ($1 + q_x$, 0, $1 + q_z$) satellite to that of the ferro-magnetic intensity (I_{FM}) at (101). In a model where the intermediate state consists of sinusoidal regions with total volume V_S, distributed equally amongst domains with each of the four observed propagation vectors, and ferromagnetic regions of total volume V_{FM} aligned along [010], we should have

$$I_S/I_{FM} = \frac{1}{16} (\mu_S^2/\mu_{FM}^2) (V_S/V_{FM}) \qquad (1)$$

where μ_S is the amplitude of the sinusoidal moment and μ_{FM} the ordered ferromagnetic moment.

We tend to favor the coexisting sinusoidal/ferromagnetic domain model over the vortex model for the following reasons: In the vortex model the intensities of each of the four satellites around a reciprocal lattice point should be the same. However, this was not the case. The intensity of one pair of satellites was roughly twice that of the other. This would be consistent with an unequal domain population in the domain model. [This incidentally, implies that the factor 1/16 in Eq. (1) is not quite correct.] There are also other difficulties such as the absence of any harmonics of the observed satellites, and the very weak temperature dependence of the periodicity of the modulated structure. If we accept the domain model, the intensity ratio of Fig. 1(a) can be interpreted as indicating that the ordered moment in the sinusoidal regions initially increases more rapidly than that in the ferromagnetic regions as the temperature is lowered. This is so because it is unlikely that the superconducting region should increase in volume relative to the ferromagnetic region once ferromagnetism sets in.

Finally, a weak external magnetic field of ~ 200 Oe was applied along the vertical [010] axis at a temperature of 0.72 K (reached on cooling). The intensity of one of the satellites and of the (101) Bragg peak was monitored. It was observed that the satellite periodicity was unchanged but that its intensity decreased from 372 counts to 204 counts (for a given number of incident neutrons), while the ferromagnetic intensity increased from 15,629 to 17,004. Using Eq. (1), and assuming that the volume lost to the modulated domains is exactly added to the ferromagnetic domains, with no change in μ_S or μ_{FM}, we obtain that at this temperature $\mu_S \approx 1.4\ \mu_{FM}$ and $V_S/V_{FM} \approx 0.2$. (The approximate signs are used because V_S is not equally divided amongst four types of domains, as discussed earlier). On switching off the external magnetic field the intensity pattern did not restore itself to the previous $H = 0$ values until the sample had been warmed up beyond T_m and recooled.

To summarize, we have shown that in a narrow temperature range $ErRh_4B_4$ exhibits both superconductivity and long-range ferromagnetic order, but in a spatially inhomogeneous manner. The superconducting regions have associated with them a transverse linearly polarized sinusoidal magnetic structure which shows apparent long-range order. The sinusoidal order parameter initially increases faster than the ferromagnetic moment, and then disappears in a strongly first order manner with decreasing temperature. The higher temperature transition between the purely superconducting and magnetically ordered phases appears to be continuous. Even weak external magnetic fields strongly suppress the modulated structure and increase the stability of the ferromgnetic phase. The wavelength of the magnetic modulation is 91.8 Å, is approximately independent of temperature below .95 K and increases to 103.5 Å at the highest temperature (0.97 K) at which it can be conveniently observed. Weak scattering from small ferromagnetic regions of size ~ 100 Å and having a volume of about 5% of the total ferromagnetic volume is also seen, and increases with the intensity of the sharp ferromagnetic peaks. The coexistence of two phases over a finite temperature region appears to be an intrinsic phenomenon rather than due to sample inhomogeneities and indicates a remarkable new pseudo-phase, namely a mosaic of microscopic superconducting and ferromagnetic regions (of size $\geq$ 2000 Å) presumably stabilized by the lowered free energy of their interfaces [15,16]. Such mixed phases have already been considered [15,16]. A slightly different possibility is that in the immediate state, a macroscopic vortex lattice exists, with a periodicity of several thousand angstroms (which cannot be resolved from a ferromagnetic peak in the present experiment) and with large flux-free superconducting regions between the fluxoid tubes in which the modulated moment exists. This would explain why the superconducting regions always stay connected down to T_{c_2} [17]. Preliminary quantitative calculations on this type of model have been reported by Hu [18].

Table I

Temp. (K)	Reflection	$\lvert F_{mag} \rvert^2$	μ_{FM}
	002	5.106	
	200	6.676	4.8 μ_B (extinction effects likely)
	101	5.310	
0.75	002	2.914	
	200	2.977	3.2 μ_B
	101	2.834	
0.95	002	0.174	
	200	*too weak to measure	0.77 μ_B
	101	0.161	
0.75	002 + $\vec{q}_s$	0.035	
	200 + $\vec{q}_s$	0.046	
	101 + $\vec{q}_s$	0.044	

REFERENCES

[1] W. A. Fertig, D. C. Johnson, L. E. DeLong, R. W. McCallum, M. B. Maple and B. T. Matthias, Phys. Rev. Letters 38 (1977) 983; B. T. Matthias, E. Corenzwit, J. M. Vandenberg and H. E. Barz, Proc. Nat. Acad. Sci. U.S.A. 74 (1977) 1334.

[2] H. R. Ott, W. A. Fertig, D. C. Johnston, M. B. Maple, and B. T. Matthias, J. Low Temp. Phys. 33 (1978) 159; H. G. MacKay, L. D. Woolf, M. B. Maple, D. C. Johnson, Phys. Rev. Letters 42 (1979). L. D. Woolf, D. C. Johnston, H. B. MacKay, R. W. McCallum and M. B. Maple, J. Low Temp. Phys. 35 (1979) 651.

[3] F. Behroozi, G. W. Crabtree, S. A. Campbell, M. Levy, D. R. Snider, D. C. Johnston and B. T. Matthias, accepted in Solid State Comm.

[4] G. K. Shenoy, B. D. Dunlap, F. Y. Fradin, S. K. Sinha, C. W. Kimball, W. Potzel, F. Probst and G. M. Kalvius, Phys. Rev. B9 (1980) 3886.

[5] D. E. Moncton, D. B. McWhan, J. Eckert, G. Shirane and W. Thomlinson, Phys. Rev. Letters 39 (1977) 1164.

[6] W. Thomlinson, G. Shirane, D. E. Moncton, M. Ishikawa and Ø. Fischer, J. Appl. Phys. 50 (1979) 1981.

[7] D. E. Moncton, D. B. McWhan, P. H. Schmidt, G. Shirane, W. Thomlinson, M. B. Maple, H. B. MacKay, L. D. Woolf, Z. Fisk and D. C. Johnston, Phys. Rev. Letters 45 (1980) 2060.

[8] E. I. Blount and C. M. Varma, Phys. Rev. Letters 42 (1979) 1079; See also M. Tachiki, A. Kotani, H. Matsumoto and H. Umezawa, Solid State Comm. 31 (1979) 927.

[9] M. Tachiki, H. Matsumoto, T. Koyama and H. Umezano, Solid State Comm. 35 (1980) 393.

[10] C. G. Kuper, M. Revzen and A. Ron, Phys. Rev. Letters 44 (1980) 1545.

[11] S. Maekawa, M. Tachiki and S. Takahashi, J. Mag. & Magn. Mat. 13 (1979) 324.

[12] H. S. Greenside, E. I. Blount and C. M. Varma, Phys. Rev. Letters 46 (1981).

[13] J. W. Lynn, A. Raggazoni, R. Pynn and J. Joffrin, J. Physique Letters 42 (1981) L45; J. W. Lynn, G. Shirane, W. Thomlinson and R. N. Shelton, Phys. Rev. Letters 46 (1981) 368.

[14] T. Riste, E. J. Samuelsen, K. Otnes and J. Feder, Solid State Comm. 9 (1971) 1455.

[15] C. M. Varma, private communication.

[16] A. J. Freeman and T. Jarlborg, J. Appl. Phys. 50 (1979) 1876.

[17] B. Patton, private communication.

[18] C. R. Hu, Bull. Am. Phys. Soc. 26 (1981) 276; C. R. Hu and T. E. Ham, Proc. of LT 16, Los Angeles, California, August 19-25, 1981.

FIGURE CAPTIONS

Fig. 1. Temperature dependence of (Q) the ferromagnetic intensity [from the (101) Bragg peak], the satellite intensity, the d.c. resistance and the ratio of the satellite to the ferromagnetic intensity for the (101) reciprocal lattice point.

Fig. 2. A high resolution diffraction scan taken through a satellite peak of the (101) Bragg reflection at 0.7 K. The FWHM of the resolution function is estimated as 0.0005 $Å^{-1}$.

Fig. 3. A scan in the vicinity of the (101) Bragg peak at 0.54 K. The scan is offset from (101) along the c* axis, and is along the a* axis. The full line is a fit of the sum of a narrow and broad Gaussian scattering function centered at (101) and folded with instrumental resolution.

Fig 1

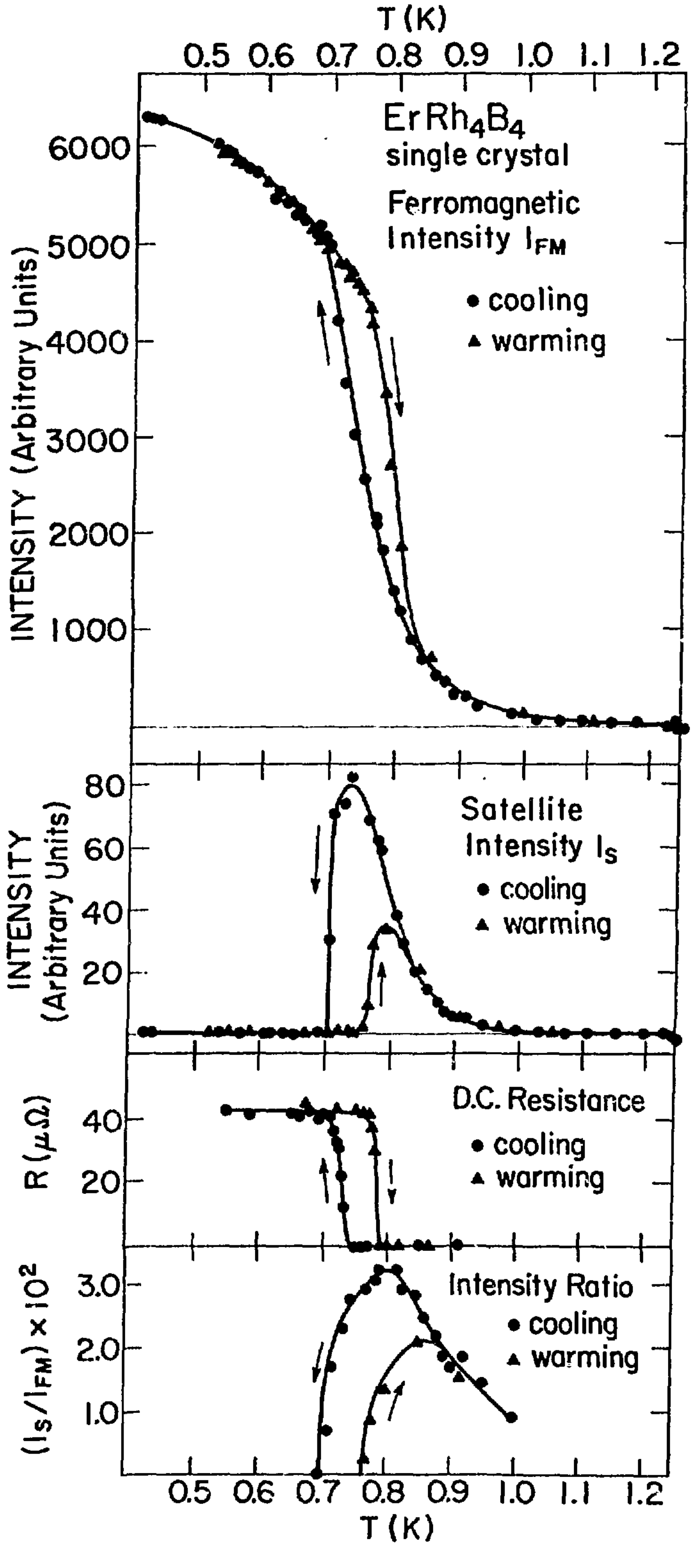

T (K)
0.5 0.6 0.7 0.8 0.9 1.0 1.1 1.2
ErRh4B4
single crystal
Ferromagnetic
Intensity IFM
• cooling
▲ warming
INTENSITY (Arbitrary Units)
6000
5000
4000
3000
2000
1000
Satellite
Intensity IS
• cooling
▲ warming
INTENSITY
(Arbitrary Units)
80
60
40
20
D.C. Resistance
• cooling
▲ warming
R (μΩ)
40
20
Intensity Ratio
• cooling
▲ warming
(IS/IFM) x 10²
3.0
2.0
1.0
0.5 0.6 0.7 0.8 0.9 1.0 1.1 1.2
T (K)

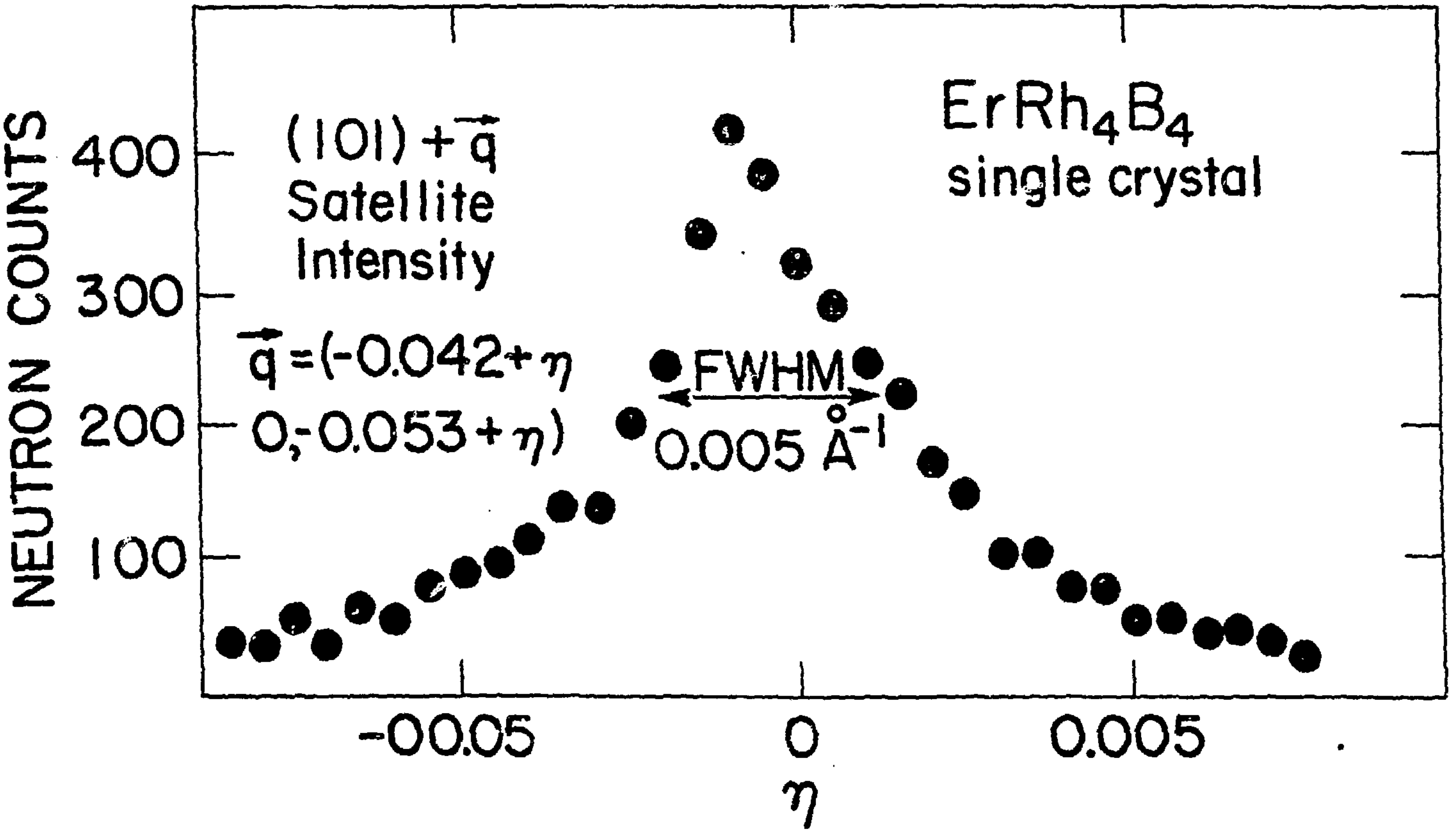
ErRh4B4
single crystal
(101) + q
Satellite
Intensity
q = (-0.042 + η
0, -0.053 + η)
FWHM
0.005 Å-1
NEUTRON COUNTS
400
300
200
100
-00.05
0
0.005
η

Fig 3

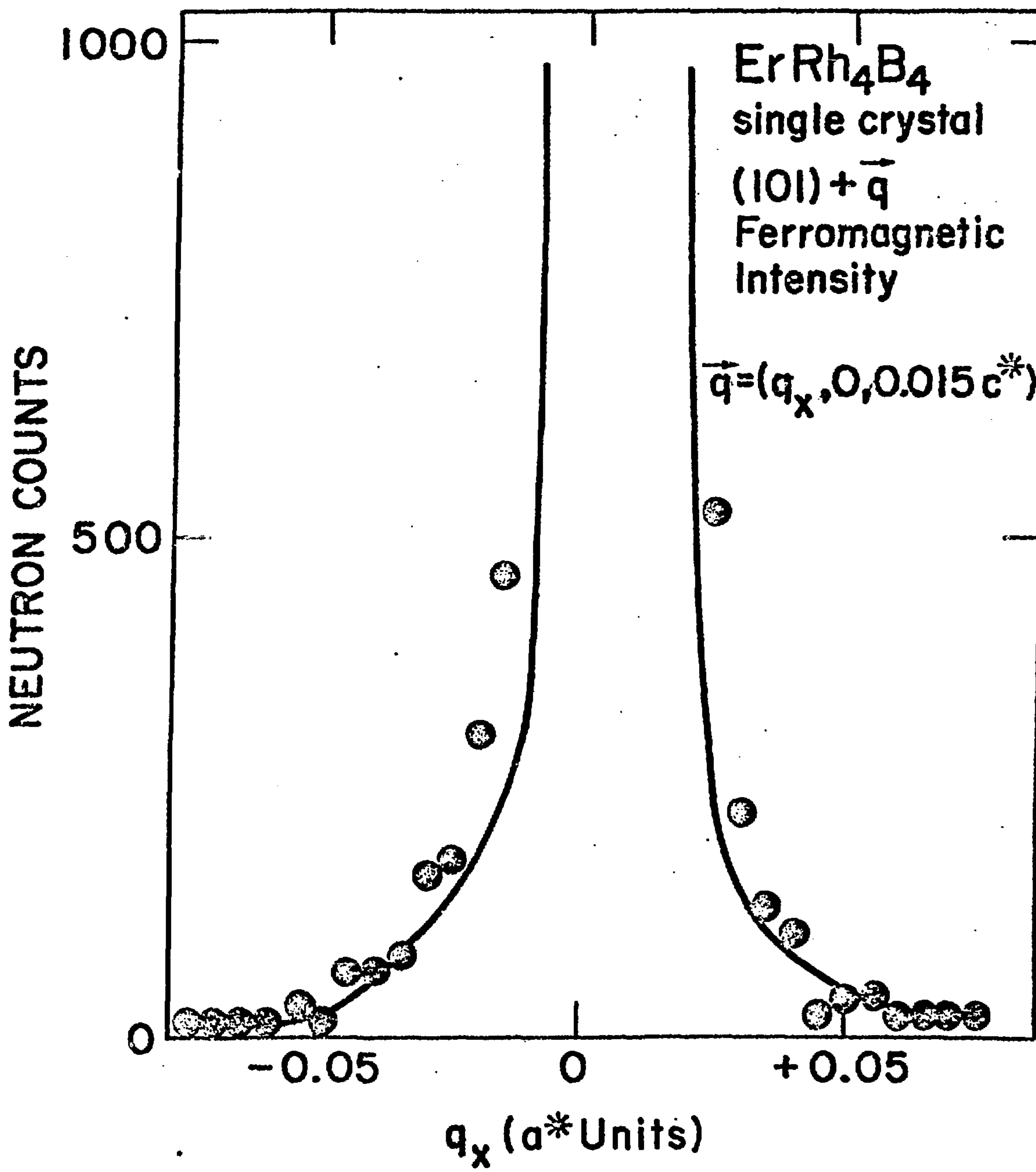

ErRh4B4
single crystal
(101) + q
Ferromagnetic
Intensity
q=(qx,0,0.015c*)
NEUTRON COUNTS
1000
500
0
-0.05
0
+0.05
qx (a* Units)

DISCLAIMER